Design space exploration through liquid H2 tank preliminary sizing and design of experiments analysis

International Journal of Hydrogen Energy xxx (xxxx) xxx

Contents lists available at ScienceDirect

International Journal of Hydrogen Energy

journal homepage: www.elsevier.com/locate/he

Design space exploration through liquid H_2 tank preliminary sizing and design of experiments analysis

Filippo Mazzoni [a,*], Roberta Biga [b], Camilo Andrés Manrique-Escobar [b], Eugenio Brusa [a], Cristiana Delprete [a]

[a] Department of Mechanical and Aerospace Engineering (DIMEAS), Politecnico di Torino, Corso Duca degli Abruzzi, 24, Torino, 10129, Italy
[b] Leonardo Innovation Labs & Intellectual Property, Leonardo S.p.A., Corso Francia 426, Torino, 10146, Italy

ARTICLE INFO

Keywords:
Preliminary design
Hydrogen storage
Aviation
Design of experiments

ABSTRACT

Energy transition towards renewable sources is essential to reduce the use of fossil fuels. To link sources and final users a flexible, available, and scalable solution must be found. Hydrogen represents the best choice being, by definition, an excellent energy carrier. The present work focuses on the aviation sector. Storage volume, critical temperature and pressure conditions, hydrogen embrittlement and boil-off phenomena are just a few of the many challenges in the design of a hybrid aircraft. The proposed analysis consists of a preliminary sizing model for a liquid hydrogen tank followed by a full-factorial design of experiments analysis. The aim of this study is to explore the design space, identifying which are the most relevant aspects, prioritizing the design parameters, and investigating their effects. These goals are reached by analyzing the quantitative data coming produced the form of chart, tables, and interaction plots. Results and observations can be useful tools to guide the engineers in understanding which areas of study are worth of greater efforts.

1. Introduction

The adoption of fossil fuels has always been increasing year after year, generating a dependency on the existing technologies that have been designed to comply with them. The urgency for developing and implementing alternative energy sources that are environmentally, economically, and socially sustainable is rapidly growing, addressing the requirement for developing systems that can harness this energy effectively. Solutions should be flexible enough to comply with many requirements coming from various industrial sectors such as heavy industry, transport, and manufacturing. Hydrogen is the best compromise. As the ideal energy vector it can store the energy coming from different resources, it can be transported through pipelines, ships or land transport systems, and can be used as fuel or converted into electricity through fuel-cells.

The aviation industry has been estimated to produce around 12% of the carbon dioxide (CO_2) emitted by the transport sector globally. Conversion of the existing aircraft is very challenging considering, for example, substituting kerosene with liquid hydrogen (LH_2) would require a four times bigger volume. On the contrary, hydrogen holds the highest energy content and has an energy density 2.5 times higher than kerosene [1–3].

One of the hardest challenges is the storage of hydrogen on board. The most common storage methods can be divided into physical-based and materials-based systems. The former consists vessels where hydrogen is stored as compressed gas at ambient conditions (CH_2), compressed gas at cryogenic temperatures (CcH_2), and in liquid form (LH_2). At the same time, the latter are typically metal or chemical hydrates to which the hydrogen is bonded and released under certain conditions of temperature and pressure or through chemical reactions [1,4,5].

Among the many storage methods, the physical-based one are the most mature, and among them, hydrogen stored in liquid form seems to be the most promising technique, at least for the near future [1,6,7]. Despite the recent interest in the use of hydrogen in aviation, studies related to H_2-powered aircraft are not new. It must be mentioned that the first feasibility studies date back to the decade 1950–1960. Between 1954 and 1957, Lockheed Aircraft Corporation, in cooperation with Pratt & Whitney Aircraft and the Rex Division of AiResearch Corporation, developed a series of conceptual designs in the context of the CL-400 aircraft project. At the same time (1955–1957), a program aimed at demonstrating the feasibility of liquid hydrogen as a fuel for both subsonic and supersonic aircraft was initiated at the NACA-Lewis Flight Propulsion Laboratory (today NASA). A B-57 twin-engine

* Corresponding author.
E-mail address: filippo.mazzoni@polito.it (F. Mazzoni).

https://doi.org/10.1016/j.ijhydene.2024.08.017
Received 7 February 2024; Received in revised form 30 July 2024; Accepted 1 August 2024

medium bomber was modified without encountering critical safety issues. Research then shifted to the space sector with the beginning of the US space program in 1958. The first successful launch of a liquid oxygen-liquid hydrogen rocket engine dates back to 1963, and in the Apollo program's following activities, the H_2 rocket propulsion system never exhibited failures. Research on hypersonic aircraft was interrupted in 1965 and restarted in 1980. Moreover, in 1988, Soviet Union flew a LH_2 Tupolev Tu-155 for about 21 min by burning hydrogen in its engines [8,9].

Still today, there are several challenges to face in the on-board H_2 storage, such as limited space available, H_2 embrittlement phenomena and cryogenic fatigue failures, systems installation to guarantee the aircraft balance throughout the flight mission, safety issues considering possible leakages, and boil-off management [10–13].

Studies in the literature investigated various aspects of the H_2 storage [8], like the LH_2 tank for small unmanned aerial vehicles [14,15], heat transfer analysis across the aircraft tank structure [16], the dynamic pressure evolution [17], the mission characteristics [10,18], and the installation requirements, for long-range and short-range aircraft concepts [19–21], for regional airliners [22,23], and for hypersonic vehicles [24,25].

H_2 storage system preliminary designs hold many design parameters and choices concerning, among others, boil-off rate (BOR), inner tank ullage, mechanical and thermal materials. The BOR maximum limit can be fixed to 20% of the idle fuel usage rate [16] as well as to 2% of the tank capacity [19], and the use of boil-off gases (BOG) as coolant can be evaluated [24]. The tank ullage is usually between 2 and 3% [22], but can also be set at 5% [26]. Compliance of mechanical and thermal materials with the operating conditions must be ensured [27]. Due to the material's well-assessed behavior and properties, the internal liner is usually made of aluminum, providing protection against H_2 permeation and a good trade-off between lightweight, strength, and toughness [22, 24]. Among the various alloys, Al5083-O is promising for its proven cryogenic behavior, H_2 compatibility, and excellent weldability [26]. Polymeric liners and liner-less tanks are also manufactured, even if their use for H_2 storage is still under research. Common insulating materials such as aerogels and low-density foams, as well as different solutions implementing vacuum jackets or multi-layer insulation (MLI) are explored [22,26,28]. In any case, the thermal layer should be capable of bearing a certain mechanical load, preventing permeability and condensations of the outer air, handling dimensional variations, apart from being lightweight and minimize the occupied volume [24].

Studies investigating the potential of hydrogen-fueled aircraft, rotorcraft, and drones are present in the literature . Saias et al. investigate the use of hydrogen to power rotorcraft. It quantifies aspects related to the design of the hydrogen storage system, referring, for instance, to the gravimetric efficiency, the energy consumption, and the CO_2 emissions, to find the optimal trade-offs and make a comparison with a kerosene fueled rotorcraft [29]. Nicolay et al. designed from scratch a fuel-cell powered general aviation. The H2 tank sizing is allocated together with the other systems inside a multidisciplinary design optimization workflow. In this case, the main design parameters of the hydrogen vessel are considered, such as the internal pressure, the filling pressure, and the ullage [30]. Onorato et al. perform the aircraft design according to a workflow where the liquid hydrogen vessel sizing is recalled at each design loop. The tank mass breakdown, geometry, and position inside the fuselage are the outputs of analysis that modify the fuselage geometry, impact the aircraft center of gravity, the load distribution and, consequently, the stability of the aircraft. Additional complexity is due to the mission profile and fuel reserve requirements affecting the mas of hydrogen to be stored, i.e. the tank characteristics, and the aircraft design parameters [31]. To identify the most significant aspect of the design of the LH2 tank and its integration inside the aircraft, Cipolla et al. developed a sizing workflow pointing out the tight connections between the parameters characterizing the storage system and those related to the aircraft sizing and mission. Non-integral tanks made of metallic structures insulated with foam are considered in the sizing loop that is iteratively launched until an optimal set of parameters leading to a successful cruise completion is found [32]. Millis et al. carry out the preliminary design of a long-endurance, high-altitude hydrogen-fueled UAV in three configurations consisting of an internal combustion engine, a solid oxide fuel cell, and a polymer exchange membrane fuel cell. The vessel thermal layer comprises vacuum-jacketed tanks with multilayer insulation, augmented with a helium pressurant system. The high amount of energy stored through the liquid hydrogen enables a mission duration from 10 to 16 days [33].

The literature also includes studies focused on more specific aspects of hydrogen storage vessels. Wank et al. analyze a tank thermal shield made of variable density multilayer insulation and hollow glass microspheres. Identifying an optimal trade-off results in considerable improvements in the vessel heat leak and in the insulation weight if compared to foam insulation [34,35]. A two-dimensional thermal model has been developed by Babac et al. to predict heat leakages by taking into account the temperature dependencies of gaseous hydrogen thermal conductivity and heat capacity. Moreover, analyzing implementing the use of a single or double vapour-cooled shield, the optimal placement leading to the minimum heat leakage is found in both scenarios [36]. Kamenimonkam et al. proposed an innovative thermal insulation design that inserted an extra layer filled with nitrogen in between the insulating foam. This intermediate layer results in an overall volume reduction, higher thermal efficiency, and enhanced robustness, apart from improving the system safety in case of hydrogen leakages that would be captured by the interaction with nitrogen. Then, the solution was implemented in the regional aircraft case study [37]. The transient heat transfer characteristics of a thermal shield made of a vapor cooled shield and multi-layer insulation are assessed and compared with the MLI-only solution in the study conducted by Jiang et al. The outputs of the study provide a deeper understanding of the solution's thermal transfer characteristic, providing useful data for further optimization of the LH_2 vessel [38]. A deeper analysis concerning the effects of the insulation thickness on the evolution of the tank pressure and thermal stratification phenomena is conducted by Joseph et al. demonstrating that a reduction in the insulation thickness leads to increases in the internal pressure rise and in the mass stratification [39]. Interesting results concerning the tank supports are provided by Xu et al. who analyze the impact of the tank supports on the heat leakages referring to a high altitude, long endurance UAV. Relying on Hertz contact theory and numerical simulations, the outputs of the analysis show a heat leak reduction of more than 85%, emphasizing the relevance of performing a detailed design for the hydrogen storage sub-systems [40].

2. Scope

Through the examination of the state of the art presented above, two main research directions emerged that are typically followed in the literature. The first one is related to the overall analysis of the aircraft, typically relying on preliminary designs, trade-off analysis, workflows or multi-disciplinary optimization solutions. From such perspectives, the inter-correlation between the H_2 storage systems on the main aspects related to the overall aircraft and flight mission are highlighted, such as the need for increasing the fuselage dimension of a general aviation aircraft to enable the tank installation or the constraints imposed by the rotorcraft structure limiting the maximum vessel size [30]. On the contrary, various publications investigate particular aspects characterizing hydrogen tanks, most of which analyze thermal engineering aspects, even though a study related to the design of tank supports has also been mentioned. The work presented here can be placed halfway between the two lines of research just mentioned, where the number of studies in the literature is more limited. Indeed, the proposed analysis aims to investigate and correlate LH_2 vessel geometrical, mechanical, and thermal aspects, neither including the model inside a specific

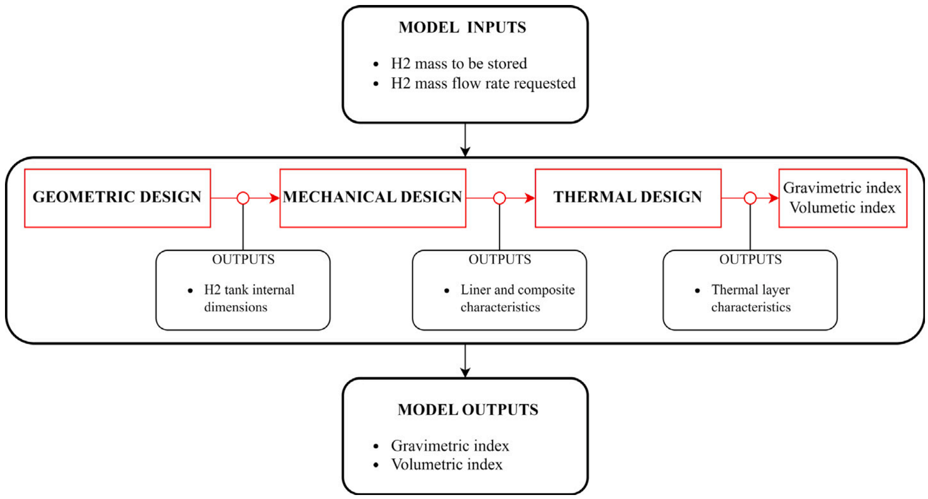

Fig. 1. Schematic of the preliminary design model.

aircraft design loop nor focusing on one or a few particular elements of the hydrogen storage system. The added values proposed here are both quantified as the LH2 vessel performances achievable depending on the inputs selected (as can be depicted in Fig. 4) and, through a Design of Experiments (DOE) analysis, quantifying the effects of most relevant design parameters on the tank performance (Figs. 5 and 6), always considering the mutual influences between geometrical, mechanical, and thermal aspects. This has been made possible by developing a parametric design model described in the following sections.

In the present work, the functional requirements to be provided by the different layers composing the tank are assumed to be H_2 permeability protection, internal pressure bearing capacity, and thermal shielding, which are satisfied by the liner, composite, and insulating layers. The outputs of the sizing model and the design of experiments (DOE) allow engineers to delineate the design space borders and the most relevant aspects worth deeper investigations.

The LH_2 tank preliminary sizing model and the full-factorial DOE herein presented aim at delineating the design space of the hydrogen storage system, paying attention to the strict weight and size constraints typical of the aviation field, thus providing an estimate of the overall tank weight and dimensions. The exploratory quantification of the main design parameters results to be relevant for both implementing existing technologies in the H_2 storing system and investigating new solutions to design innovative architectures.

Considering both the cryogenic conditions that must be assured to store liquid hydrogen and the numerous contributions in the literature investigating different topics related to thermal design, tank insulation is expected to play a relevant role in the overall vessel design. However, several issues have to be clarified. The definition of a design road map must be bolstered by quantifying the expected outcomes to prioritize the various design parameters properly and the further activities to be performed.

In summary, the scope of the present analysis is to provide quantitative data to understand and prioritize the main design parameters, analyze their influence on the gravimetric and volumetric indexes, which are considered among the most important factors for the design of hydrogen storage tanks, so to provide the engineer with preliminary results useful in the choice of further design steps.

3. Methodology

The design is implemented through a Python modeling script that performs the preliminary sizing of a tank consisting of a composite mechanical structure enveloped by an insulation layer. The model is then processed through a full-factorial DOE aiming to understand the relevance of selected parameters through their influences on the outputs.

3.1. Design model

A schematic of the model is reported in Fig. 1. The tank sizing is divided in three steps: geometric, mechanical, and thermal designs, which will be described below. The final outputs are the gravimetric and volumetric indexes, that are used as performance parameters to compare the different solutions, and are reported in the following formulas:

$$grav_{index} = \frac{m_{H_2}}{m_{H_2} + m_{tank}} \qquad (\%) \tag{1}$$

$$vol_{index} = \frac{V_{H_2}}{V_{tank}} \qquad (\%) \tag{2}$$

The gravimetric index (Eq. (1)) is the ratio between the mass of hydrogen stored and the sum of the full tank (sum of the H_2 mass stored plus the empty tank mass). Higher gravimetric indices are always one of the main design goals as they increase the aircraft payload.

The volumetric index (Eq. (2)) is the ratio between the volume occupied by the stored hydrogen and the total tank volume. Holding high volumetric index results in less space occupied by the H_2 tank and, in some cases where the aircraft structure needs to be modified, in better aerodynamic profiles and lower fuel consumption.

3.1.1. Geometric design

The tank geometry is constrained to a cylindrical central body with hemispheric caps. This choice has been taken to maximize the area-to-volume ratio (AVR) and guarantee considerable accuracy of the mechanical model implemented. Holding a low AVR turns out to be advantageous because it allows a lower heat exchange surface for equal tank capacities, thus reducing the insulation material needed and the tank weight. The geometric script has been parameterized according to the diameter-over-length ratio β (Eq. (3)), which modifies the geometry ranging from a sphere (β= 1) to a long and thin vessel shape (β tending to zero). A qualitative example of the tank shape for varying β is reported in Fig. 2.

$$\beta = D/L \qquad (-) \tag{3}$$

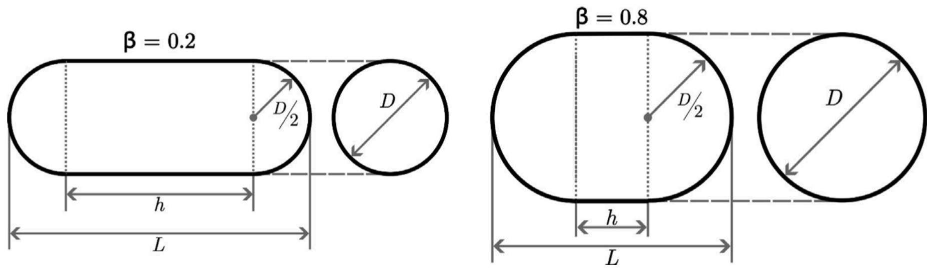

Fig. 2. Tank geometry for varying β (diameter-over-length ratio).

3.1.2. Mechanical design

The tank mechanical structure is a composite vessel made of an internal aluminum liner of 2 mm thickness, enveloped by continuous high tensile strength carbon fiber composite material, with a fraction of fiber volume (V_f), also called fiber-to-volume ratio, of 0.6. The mechanical design has been performed according to ISO 11439 (2000) and ASME Sec. X (2004) standards [41]. It is assumed that the metal liner does not bear any load, and its purpose is to avoid hydrogen permeability through the tank wall [42]. The epoxy resin is also assumed not to bear any mechanical load. Due to manufacturing weldability limitations, the liner thickness was set at 2 mm. The minimum composite thickness has been fixed here at 1.6 mm, mainly for manufacturability limits, which approximately correspond to the two composite layers that were deposited. If the resulting layer thickness is lower than that determined value, the model automatically sets it at the lower limit.

The so-called burst safety coefficient is defined in Eq. (4). It applies under static behavior and it is a safety factor expressed as the ratio between burst pressure (p_b: pressure that the vessel can handle before rupture) and service pressure (p_s: maximum pressure at which hydrogen is stored during operations).

$$\frac{p_b}{p_s} \geq 2.35 \tag{4}$$

The composite layer is made of alternating hoop and helical winding, and the total composite thickness is the sum of both contributions computed by Eqs. (5) and (6), respectively.

$$t_{\text{tot,layer,hoop}} = \frac{p_b \cdot R_C}{\sigma_{cr,fib} \cdot V_f}\left[1 - \frac{1}{2}\tan^2(\alpha_c)\right] \quad (m) \tag{5}$$

$$t_{\text{tot,layer,helical}} = \frac{p_b \cdot R_C}{2 \cdot SR \cdot \sigma_{cr,fib} \cdot V_f \cdot \cos^2(\alpha_c)} \quad (m) \tag{6}$$

where p_b (MPa) is the burst pressure, R_C (m) the cylinder radius, $\sigma_{cr,fib}$ (MPa) is the fiber ultimate strength, V_f (-) the fraction of fiber volume, and α_c (degrees) is the cylinder fiber angle, i.e., the angle between fiber and longitudinal cylinder direction. The values of α_c are assumed equal to 90° and 45° for the hoop and helical winding, respectively.

3.1.3. Thermal design

Fig. 3 shows a schematic of the thermal equivalent circuit implemented. The phenomena considered are natural convection between the tank's outer layer and the external environment and conduction through the thermal and mechanical layers. The heat entering is assumed to be fully absorbed by the liquid H_2 at full tank conditions and converted into boil-off gases. Being the tank non-integral, the thermal contribution coming from radiation is neglected. Internal convection between the liquid H_2 and the vessel's inner wall and interactions between the H_2 gaseous and liquid phases are also neglected, being not the main focus of the present work.

The schematic shown in Fig. 3 is translated analytically through Eq. (7) [43].

$$Q_{in} = \frac{T_{ext,env} - T_{int,surface}}{\frac{\ln\frac{r_{inner}}{r_{ext,liner}}}{2\pi k_{liner} L} + \frac{\ln\frac{r_{in,comp}}{r_{ext,comp}}}{2\pi k_{comp} L} + \sum_{i=1}^{n}\frac{\ln\frac{r_{in,th,i}}{r_{ext,th,i}}}{2\pi k_i L} + \frac{1}{2\pi r_{ext,n} L h_{ext,env}}} \tag{7}$$

where Q_{in} (W) is the heat entering the tank, $T_{ext,env}$ (K) is the temperature of the external environment (computed as: ISO+35 °C = 50 °C), and $T_{int,surface}$ (K) is the temperature of the internal tank surface. r_{in} (m) is the internal radius of a layer while r_{ext} (m) is the external one. k (W/m K) represents the thermal conductivity, L (m) the cylinder length, and $h_{ext,env}$ (W/m^2 K) the external natural convection coefficient. Subscripts in Eq. (7) parameters refer to the different layers, also shown in Fig. 3.

To provide the model with a certain degree of flexibility, the heat incoming through external convection is automatically computed for both spherical and cylindrical shapes, and the worst case is selected. Still, the liquid hydrogen properties are calculated along the saturation curve according to the worst-case scenario.

$$BOR = \frac{Q_{in} \cdot 24 \cdot 3600 \cdot 10}{V_{LH_2} \cdot \rho_{LH_2} \cdot H_{vap} \cdot 100} \tag{8}$$

Eq. (8) is implemented to compute the BOR in (%/h). V_{LH_2} (m^3), ρ_{LH_2} (kg/m^3) and H_{vap} (J/kg) are, respectively, volume, density and H_2 latent heat of vaporization.

3.2. Full factorial DOE

A two-level full-factorial DOE has been executed to observe the influence of four independent parameters (control factors) on two outputs selected: gravimetric and volumetric indices. Additionally, two noise factors, the external temperature and pressure corresponding to the ambient conditions inside the fuselage, have been artificially added to analyze their effect and evaluate the advantages of designing an environment-controlling system [44,45]. The control and noise factors reported in Table 1 are the venting pressure p_{vent}, the additional H_2 mass stored as a safety margin $m_{H_2,SM}$, the thermal layer thickness $t_{thermal}$, diameter-over-volume ratio β, the environmental temperature T_{env}, and p_{env} representing the environmental pressure. Such parameters have been analyzed here because they have to be defined by the engineer during the design phase. The values of other parameters in the sizing model are constrained by standards. Thus, their influence on the final outputs has been considered less relevant.

The maximum and minimum levels reported in Table 1 have been selected relying on technical considerations derived from the literature research already described in Section 1, and from the analysis of the sizing model previously introduced in Section 3. The p_{vent} can be defined as the maximum service pressure above which gaseous H_2 is expelled from the tank to keep the internal pressure level below a maximum. The value of p_{vent} is typically driven by two issues: the natural tendency of liquid hydrogen density to decrease for increasing pressures and the vessel internal pressure that must be higher than the outer pressure to avoid air entering the vessel in case of small cracks or failures of certain components. So, the p_{vent} is usually set at a level slightly higher than the outer pressure. In the present analysis, to evaluate whether investing a considerable amount of time in a very careful and deep analysis of the choice of p_{vent} is worthwhile, the lower level has been set equal to the environmental pressure at sea level (0.1 MPa), while the upper one is at 1 MPa.

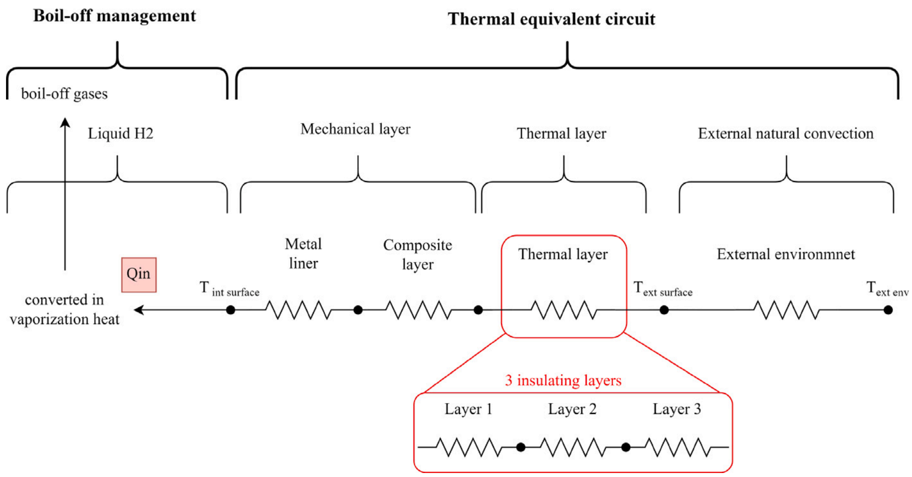

Fig. 3. Electric-thermal resistance circuit analogous.

$m_{H_2,SM}$ is the quantity of hydrogen additionally stored, represented as the percentage increase in addition to that requested by the user, to account for boil-off losses and fuel reserve. Selecting a higher safety margin means storing more hydrogen, thus more weight, but also a higher quantity of hydrogen can be lost due to boil-off, which translates to higher heat leakages and lighter thermal insulation. The optimal trade-off between the two scenarios requires dynamic analysis and life-cycle assessments, apart from depending on the aircraft type and the mission requirements, thus going beyond the scope of this work. The upper and lower levels of $\Delta\ mH_{2,SM}$ have thus been set to the minimum and maximum levels typically present in the literature.

To quantify the influence of the vessel geometry, the β factor levels have been selected as the extremes of the widest possible range. Indeed, a β value of 1 corresponds to a spherical shape, representing a good benchmark for comparison even though it is difficult to manufacture. In contrast, a β equal to 0.2 is characteristic of a long and slim vessel. Values below 0.2 have not been found in the literature.

The levels of the thermal layer thickness have been set starting from the outputs of the sizing model presented in Fig. 4. The lower and upper levels of $t_{thermal}$ equal to 90 mm and 710 mm correspond to generated boil-off rates of 1% and 5%, respectively. Such a range of the boil-off rate has been evaluated as a good trade-off among the maximum admissible losses (5% BOR) and a minimum value (1% BOR), below which further increasing $t_{thermal}$ does not significantly reduce the heat entering the tank.

Lower environmental pressures and higher outer temperatures should be unfavorable for the tank's performance. Indeed, increasing in the difference between internal and external pressure should result in a thicker and heavier mechanical structure. Similarly, higher outer temperatures require a thicker $t_{thermal}$ to limit the BOR below the maximum admissible level. According to this reasoning, T_{env} upper level has been set from ASHRAE standard as the maximum hot day temperature on the ground (50 °C [46]), while the p_{env} at 0.01 MPa, corresponding to the ambient pressure at an altitude of around 50000 feet, above the level most commercial aircraft fly. These two conditions have been identified as the worst-case scenarios referring to the external environmental conditions. The T_{env} lower level and the p_{env} upper level, set equal to the standard temperature and pressure conditions (0 °C, 1 bar [47]), are considered of minor importance for the current investigation due to their positive effect on the tank performance.

The numeric outputs computed for all the possible combinations are reported in Table 2. Even though the gravimetric and volumetric indexes are the mean among those computed at the different noise factors levels ($grav_{index,mean}$ and $vol_{index,mean}$), the effect of noises has been considered negligible and not reported.

Table 1
Full-factorial parameters levels.

Level	Control factors				Noise factors	
	p_{vent} (MPa)	$\Delta\ mH_{2,SM}$ (%)	β (–)	$t_{thermal}$ (m)	T_{env} (K)	p_{env} (MPa)
Level 1	0.1	+ 2	0.2	0.09	273.15	0.01
Level 2	1	+ 20	1	0.71	323.15	0.1

4. Results

In the following, results from the preliminary sizing of the H_2 tank and the design of experiments analysis have been investigated. Apart from examining the different outputs separately, it is also interesting to observe them together, trying to identify the common elements and providing a further added value.

4.1. Design model results

Fig. 4 shows a summary of the main outputs coming from the tank sizing model. As it will be shown in the section below, the thermal layer thickness ($t_{thermal}$) is one of the main drivers for the tank design and it is here plotted along the *x*-axis. This is in agreement with the authors' expectations. Indeed, the tank performances depend on the weight and volume of the mechanical and thermal layers, which, in turn, are functions of the internal pressure load and the heat entering the vessel. However, the mechanical loads are relatively low, and variations of the internal pressures below ten bars, that are typical of LH_2 vessels, do not considerably affect the tank structure. On the other hand, the cryogenic conditions at which the liquid hydrogen must be stored make the thermal design crucial. In Fig. 4, the multiple y-axes report, from left to right, the heat entering through the tank wall that, considering the previous assumption, corresponds directly to the boil-off gases generated, the empty tank weight, the gravimetric index, and the volumetric index. It can be immediately depicted how changes in the $t_{thermal}$ lead to dramatic variations of all the parameters just mentioned, substantiating the reasoning proposed above.

System weight and size are of fundamental importance in the aviation field. These are described in Fig. 4 through the gravimetric and volumetric indexes ($grav_{index}$ and vol_{index}) that exhibit a similar trend throughout all the thermal layer thicknesses. As expected, the empty tank weight (m_{tank}) follows an opposite trend with respect to the $grav_{index}$. In blue, the heat through the tank wall (Q_{in})shows a steep decrease for a $t_{thermal}$ spanning from 0 to approx. 0.1 m. Then, the curve starts flattening, and the trend becomes asymptotic for a thermal thickness greater than 0.6 m.

Table 2
Full factorial plane with mean results.

No.	p_{vent} (MPa)	$m_{H_2,SM}$ (%)	β (–)	$t_{thermal}$ (m)	$grav_{index,mean}$ (%)	$vol_{index,mean}$ (%)
1	–	–	–	–	42.06	61.56
2	–	–	–	+	4.30	9.18
3	–	–	+	–	51.45	68.91
4	–	–	+	+	9.75	12.38
5	–	+	–	–	43.59	63.00
6	–	+	–	+	4.79	9.97
7	–	+	+	–	52.91	70.20
8	–	+	+	+	10.63	13.41
9	+	–	–	–	42.06	61.56
10	+	–	–	+	4.30	9.18
11	+	–	+	–	51.45	68.91
12	+	–	+	+	9.75	12.38
13	+	+	–	–	43.59	63.00
14	+	+	–	+	4.79	9.97
15	+	+	+	–	52.91	70.20
16	+	+	+	+	10.63	13.41

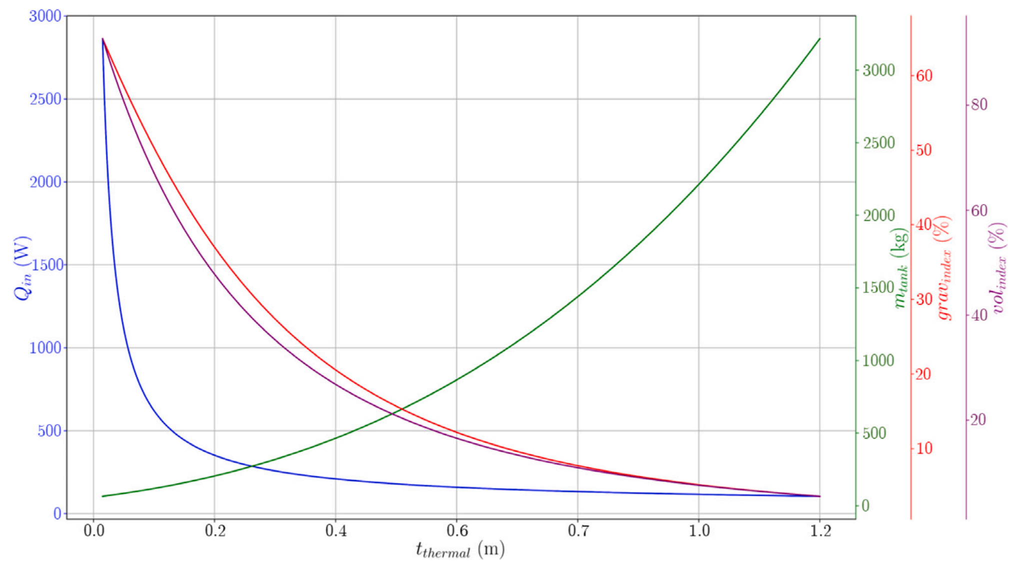

Fig. 4. Relation between the thermal layer thickness ($t_{thermal}$), the heat entering the tank (Q_{in}, in blue), the empty tank mass (m_{tank}, in green), the gravimetric index ($grav_{index}$, in red), and the volumetric index (vol_{index}, in purple).

If no particular constraints are imposed, it may seem that the range of $t_{thermal}$ worth of further investigations would be approximately between 100 and 500 mm. For aircraft applications, however, a BOR ranging from 5 to 1% percent has been considered reasonable considering a typical profile mission and the idle times before takeoff and after landing. These values correspond to an insulation thickness between 90 and 710 mm. Such range has been further investigated and correlated with other sizing parameters through the full-factorial design of experiments.

4.2. DOE results

The interaction plots in Figs. 5 and 6 exhibit an overall similar trend. The thermal layer thickness is dominant in both cases. The β still holds a non-negligible influence, higher for the gravimetric index. Storing an additional quantity of H_2 up to 20% of the tank capacity increases the gravimetric and volumetric indexes by a few percentage points. Finally, the effect of venting pressure can be assumed negligible, coherently with the previously made assumptions, and considering that the carbon-fiber composite tank does not sense a pressure difference for such low values.

Overall, based on the various design choices, it can be observed that the gravimetric index can range from 5 to 50%, while the volumetric index ranges from 10 to almost 70%. Furthermore, the effects coming from the noise factors, namely the venting pressure and the external ambient temperature, have been considered negligible and have not been reported here.

A numerical quantification of the trend shown in Figs. 5 and 6 can be seen in Tables 3 and 4, respectively. Again, the relevance of the four control factors can be estimated by looking at the last two rows of each table. Focusing on the mean gravimetric index (computed by averaging the values of the $grav_{index,mean}$ in Table 2, and reported in Table 3), passing from level 1 to 2 it has been observed an increase of 4.05% for the $m_{H_2,SM}$, of 31.69% for the β, and a decrease of 84.49% for the increasing $t_{thermal}$. Analogously, observing the effects on the mean volumetric index (Table 4), increases of 3% and 14.75% result for the $m_{H_2,SM}$ and the β, respectively. A decrease of 82.95% corresponding to the increment in $t_{thermal}$ is detected.

5. Discussion

The previous sections identified the main aspects related to hydrogen storage system design, allowing the designer to substantiate initial expectations, provide useful inputs to link the hydrogen vessel sizing with the overall aircraft design and quantify the influence of the main design factors. The thermal layer thickness ($t_{thermal}$) results in the predominant parameter among those investigated in the DOE, meaning that particular attention must be devoted to the design of

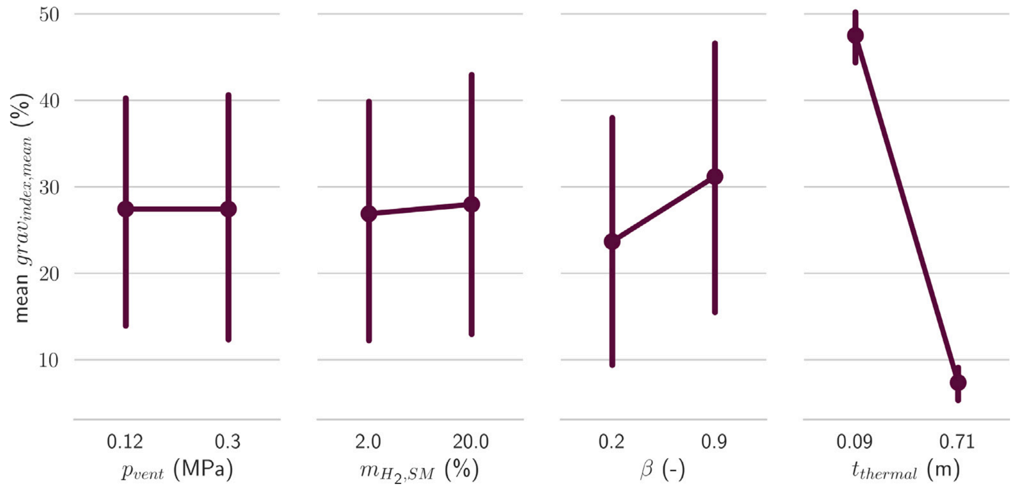

Fig. 5. Gravimetric index interactions plot.

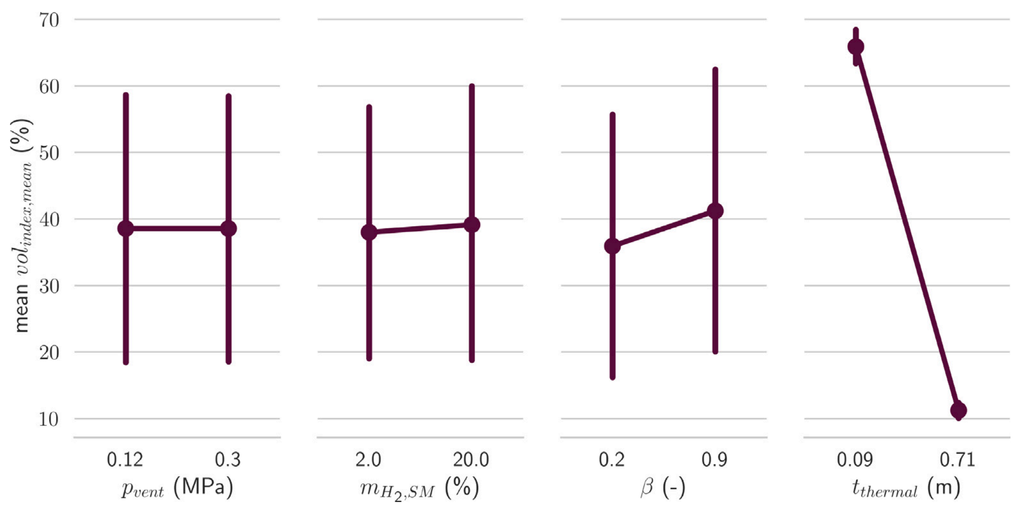

Fig. 6. Volumetric index interactions plot.

Table 3
ANOVA table for mean gravimetric index.

		p_{vent}	$m_{H_2,SM}$	β	$t_{thermal}$
mean $grav_{index,mean}$	Level 1	27.44	26.89	23.68	47.50
	Level 2	27.44	27.98	31.19	7.37
	Sum of squares	0.00	1.19	56.32	1610.95
	dof	1	1	1	2
	Variance factor	0.00	1.19	56.32	805.48
	Percentage weight	0.00%	0.14%	6.53%	93.34%

Table 4
ANOVA table for mean volumetric index.

		p_{vent}	$m_{H_2,SM}$	β	$t_{thermal}$
mean $vol_{index,mean}$	Level 1	38.58	38.01	35.93	65.92
	Level 2	38.58	39.15	41.23	11.24
	Sum of squares	0.00	1.30	28.08	2989.94
	dof	1	1	1	1
	Variance factor	0.00	1.30	28.08	2989.94
	Percentage weight	0.00%	0.04%	0.93%	99.03%

the thermal layer, which strongly influences both the gravimetric and volumetric indexes. More detailed values can also be depicted in Fig. 4. The vessel geometry, expressed through the β factor, the ratio between the tank length and the tank diameter, also plays an important role. β values tending to one, corresponding to shorter and stockier vessels, are preferable. Larger quantities of hydrogen stored result in vessels holding higher gravimetric and volumetric indexes, as highlighted by the results obtained for different values of the additional mass of H_2 stored as safety margin ($m_{H_2,SM}$). Instead, no relevant effects varying the venting pressure (p_{vent}) have been observed.

It must be specified that the trends just delineated are bounded by the limits of the sizing model and the scope of the proposed study. Indeed, the tank geometry is strictly correlated with installation requirements and fuselage dimensions. At the same time, the $m_{H_2,SM}$ strongly depends on the aircraft type and mission profile, and its correct estimation would also require a life-cycle analysis. The values of $t_{thermal}$ are provided under the assumption of non-integral tanks, even if integral tanks typically hold better performance but require a complete knowledge of the aircraft structure. In addition, the sizing model implemented here performs static analysis and does not consider the structural characteristics of the insulating material, which, being the outermost shell, should also be capable of bearing at least the weight of the full tank itself.

Despite the intrinsic limitations of the sizing model, the major contributions of the current study still hold. The main objective of the design exploration is to guide further design steps through qualitative and quantitative analysis. The results plotted in Fig. 4, together with the outcomes of the DOE, are useful both to prioritize the design factors and as a measure of validation for subsequent analysis.

Further developments include implementing features that make the model capable of including vessels with semi-elliptical caps geometries, mechanical layers made of polymers and metals, and thermal shields built of different materials and multiple layers. Then, optimal solutions can be identified and used as the starting point for following dynamic analysis. For a given aircraft's characteristics, the mechanical and thermal design can be coupled, and, for instance, the tank thermal behavior can be deeply investigated, characterizing fluid sloshing and pressure variations phenomena. Moreover, the integration between the H_2 vessel and the aircraft can be inspected. Due to the high volumes and the technological complexity of managing hydrogen at cryogenic temperatures, system integration is one of the main concerns in the overall design of hybrid-electric aircraft, and this must be assessed in further design steps.

6. Conclusion

The work proposed here can be located between the two main research areas. The first research area comprises studies that analyze a whole aircraft, thus considering the hydrogen storage tank as an element of a greater system. In contrast, the second research area focuses on more detailed aspects of the hydrogen storage system, such as the insulation or the supports, thus not considering the storage vessel as a whole.

This study proposes a preliminary sizing of a liquid hydrogen tank followed by a full-factorial DOE. The sizing model consists of three parts (Fig. 1). Geometric design defines the tank shape starting from the mass of hydrogen required by the fuel cell. Based on the required operating pressures, mechanical design computes the thickness, weight and volume of the metal liner and the carbon fiber composite, and thermal design provides the thickness and weight of the insulating material as a function of the requested boil-off rate. The model is then further analyzed through a full-factorial design of experiments, providing the engineer with relevant information about the priority of selected design factors and representing a guideline indicating which aspects are worth deeper investigation along the subsequent design steps.

The sizing model outputs highlight the relevance of thermal insulation as the main driver for the design. Fig. 4 immediately shows a design area corresponding to the variation in curvature of the heat trough tank wall. This relevant area can be further delineated by correlating the entering heat with the permissible boil-off rate, as has been done in Section 4.1, resulting in a thermal insulation thickness between 90 and 700 mm that, in turn, also depends on the specific aircraft needs. The composite layer does not sense the difference in the operating pressures imposed, which are relatively low throughout the range. The DOE analysis also proves the relevance of the insulating layer. Interaction plots in Fig. 5 and Fig. 6 show the gravimetric and volumetric indices spanning 5 – 50% and 10 – 70%, respectively. The effects of venting pressure are negligible. These results are reasonable with the model's assumption that automatically limits the composite layer thickness to a lower bound, which is assumed to be the manufacturability limit. Composite pressure vessels are meant to work at higher pressures than those considered in the present work. Thus, the model assigns a minimum value to the composite thickness regardless of the range of p_{vent} analyzed. Increasing the H_2 mass safety margin, both the gravimetric and volumetric indices increase, pointing out that storing a greater quantity of hydrogen is advantageous both in terms of space occupied and system mass, even if a trade-off analysis taking into account the aircraft fuel consumption and the drag forces should be conducted. The benefits of changing the tank geometry towards a shorter and thicker shape have been estimated in gravimetric and volumetric indices increases around 30% and 15%, respectively.

The findings and limitations resulting from the present study can be interpreted to define which design pathways are worth pursuing. Improvement in the LH_2 tank geometry should not be conducted as a stand-alone activity. The tight connections with aircraft dimensions, installation requirements, balance of masses, and fuselage structure, apart from manufacturability limitations, pose several constraints to the choice of the most suitable tank geometry. Moreover, increasing efforts and studies in materials science will produce innovative polymers, alloys, and thermal insulators. It is then appropriate to enhance the model's features to include different geometrical, mechanical, and thermal solutions to keep up with technological developments. Limitations are imposed by the nature of the model itself, which can only analyze one-dimensional static phenomena. To further investigate the vessel's thermal behavior, which is identified as one of the most important aspects, dynamic models must be developed and correlated to an aircraft type, i.e., specific characteristics and mission profile. By implementing a use case and developing a time-dependent analysis, the thermo-mechanical and thermal fatigue coupled phenomena can be investigated.

The DOE highlighted a hierarchy among the parameters selected, suggesting the priorities that can be assigned to the different aspects. Results show that, at the preliminary level, the design of the thermal layer is the most relevant, the geometrical design is still important, and the mechanical design has the lowest influence on the outputs, namely gravimetric and volumetric indexes. However, it is worth mentioning that, depending on the set of parameters analyzed, the effect of factors holding a lower influence on the outputs can be hidden by those having a predominant effect. Therefore, the DOE analysis should be iteratively applied to a set of properly selected parameters as the design increases in detail.

Outlining future perspectives, two main directions worth pursuing arise. The first is related to the interaction and integration of the hydrogen storage vessel with the aircraft and the other onboard systems, suggesting that applying a proper methodology, such as Model-Based Systems Engineering, harmonizes all the functional and logical properties through suitable architectures. The second direction concerns the modeling of different phenomena. Further developments include the simulation of tank mechanical and thermal dynamic behaviors, fluid sloshing, and gas stratification, apart from thermal and mechanical coupled fatigue phenomena.

Summarizing, it is clear how further investigations must always be integrated and never conducted as stand-alone activities. The hydrogen storage system is fundamental for the design of hybrid-electric aircraft. Integration must be the common thread among the various aspects and be reflected in further model developments.

CRediT authorship contribution statement

Filippo Mazzoni: Writing – review & editing, Writing – original draft, Visualization, Validation, Software, Methodology, Investigation, Formal analysis, Data curation, Conceptualization. **Roberta Biga:** Writing – review & editing, Supervision, Methodology, Conceptualization. **Camilo Andrés Manrique-Escobar:** Writing – review & editing, Supervision, Methodology, Conceptualization. **Eugenio Brusa:** Writing – review & editing, Validation, Supervision, Methodology, Formal analysis, Conceptualization. **Cristiana Delprete:** Writing – review & editing, Validation, Supervision, Methodology, Formal analysis, Conceptualization.

Declaration of competing interest

The authors declare that they have no known competing financial interests or personal relationships that could have appeared to influence the work reported in this paper.

Acknowledgments

The authors acknowledge Politecnico di Torino and Leonardo S.p.A. for the collaboration and the continuous support.

References

[1] Baroutaji A, Wilberforce T, Ramadan M, Olabi AG. Comprehensive investigation on hydrogen and fuel cell technology in the aviation and aerospace sectors. Renew Sustain Energy Rev 2019;106:31–40. http://dx.doi.org/10.1016/j.rser.2019.02.022.

[2] Oesingmann K, Grimme W, Scheelhaase J. Hydrogen in aviation: A simulation of demand, price dynamics, and CO2 emission reduction potentials. Int J Hydrog Energy 2024;64:633–42. http://dx.doi.org/10.1016/j.ijhydene.2024.03.241.

[3] Contreras A, Yiğit S, Özay K, Veziroğlu TN. Hydrogen as aviation fuel: A comparison with hydrocarbon fuels. Int J Hydrog Energy 1997;22(10):1053–60. http://dx.doi.org/10.1016/S0360-3199(97)00008-6.

[4] Boretti A, Huang A. Physical storage in conformal composite tanks presents clear advantages over material-based solutions for hydrogen-powered aerospace applications. Int J Hydrog Energy 2024;68:1297–301. http://dx.doi.org/10.1016/j.ijhydene.2024.04.258.

[5] Mehr AS, Phillips AD, Brandon MP, Pryce MT, Carton JG. Recent challenges and development of technical and technoeconomic aspects for hydrogen storage, insights at different scales; A state of art review. Int J Hydrog Energy 2024;70:786–815. http://dx.doi.org/10.1016/j.ijhydene.2024.05.182.

[6] Otto M, Chagoya KL, Blair RG, Hick SM, Kapat JS. Optimal hydrogen carrier: Holistic evaluation of hydrogen storage and transportation concepts for power generation, aviation, and transportation. J Energy Storage 2022;55:105714. http://dx.doi.org/10.1016/j.est.2022.105714.

[7] Prewitz M, Schwärzer J, Bardenhagen A. Potential analysis of hydrogen storage systems in aircraft design. Int J Hydrog Energy 2023;48(65):25538–48. http://dx.doi.org/10.1016/j.ijhydene.2023.03.266.

[8] Brewer G. Hydrogen aircraft technology. 1st ed.. United Kingdom: Routledge; 2017, http://dx.doi.org/10.1201/9780203751480.

[9] Pohl HW, Malychev VV. Hydrogen in future civil aviation. Int J Hydrog Energy 1997;22(10):1061–9. http://dx.doi.org/10.1016/S0360-3199(95)00140-9.

[10] Sarkar S, Grandi G, Patel S. Hydrogen Fuel System for Aircraft. In: SAE technical papers. 2023, http://dx.doi.org/10.4271/2023-01-0976.

[11] Nuwantha HDN, Jung D, Huh C. Improvement in predicting the thermal behavior of liquid hydrogen storage through novel thermal modeling. Int J Hydrog Energy 2024;72:1143–58. http://dx.doi.org/10.1016/j.ijhydene.2024.05.382.

[12] Vietze M, Weiland S. System analysis and requirements derivation of a hydrogen-electric aircraft powertrain. Int J Hydrog Energy 2022;47(91):38793–810. http://dx.doi.org/10.1016/j.ijhydene.2022.09.052.

[13] Oh SJ, Kwon J, Jeon KS, Yoon JH. A numerical analysis study on the characteristics of evaporation in liquid hydrogen tank with vacuum layer according to changes in heat flux and vacuum pressure. Int J Hydrog Energy 2024;50:542–57. http://dx.doi.org/10.1016/j.ijhydene.2023.07.271.

[14] Swider-Lyons K, Stroman R, Rodgers J, Edwards D, Mackrell J, Schuette M, Page G. Liquid hydrogen fuel system for small unmanned air vehicles. In: 51st AIAA aerospace sciences meeting including the new horizons forum and aerospace exposition 2013. 2013.

[15] De Wagter C, Remes B, Smeur E, van Tienen F, Ruijsink R, van Hecke K, van der Horst E. The *NederDrone*: A hybrid lift, hybrid energy hydrogen UAV. Int J Hydrog Energy 2021;46(29):16003–18. http://dx.doi.org/10.1016/j.ijhydene.2021.02.053.

[16] McFarland C, Agarwal RK. A simple model of thermal insulation design for cryogenic liquid hydrogen tank. 2022.

[17] Rahman AA, Wang H, Wang B, Xu T, Li J, He Y, Jin T, Gan Z. Prediction of pressure evolution in non-venting self-pressurized liquid hydrogen tanks using artificial neural network approach. Int J Hydrog Energy 2024;68:428–39. http://dx.doi.org/10.1016/j.ijhydene.2024.04.261.

[18] Rompokos P, Rolt A, Rolt A, Sibilli T, Benson C. Cryogenic fuel storage modelling and optimisation for aircraft applications. In: Proceedings of the ASME turbo expo. Vol. 6, 2021, http://dx.doi.org/10.1115/GT2021-58595.

[19] Xisto C, Lundbladh A. Design and performance of liquid hydrogen fuelled aircraft for year 2050 EIS. In: 33rd congress of the international council of the aeronautical sciences. ICAS 2022, Vol. 2, 2022, p. 1119–31.

[20] Jagtap SS, Childs PRN, Stettler MEJ. Performance sensitivity of subsonic liquid hydrogen long-range tube-wing aircraft to technology developments. Int J Hydrog Energy 2024;50:820–33. http://dx.doi.org/10.1016/j.ijhydene.2023.07.297.

[21] Burschyk T, Cabac Y, Silberhorn D, Boden B, Nagel B. Liquid hydrogen storage design trades for a short-range aircraft concept. CEAS Aeronaut. J. 2023;14(4):879–93. http://dx.doi.org/10.1007/s13272-023-00689-4.

[22] Verstraete D, Hendrick P, Pilidis P, Ramsden K. Hydrogen fuel tanks for subsonic transport aircraft. Int J Hydrog Energy 2010;35(20):11085–98. http://dx.doi.org/10.1016/j.ijhydene.2010.06.060.

[23] Bai M, Yang W, Yan J, Zhang R, Qu Z. Cryogenic turbo-electric hybrid propulsion system with liquid hydrogen cooling for a regional aircraft. Int J Hydrog Energy 2024;71:541–61. http://dx.doi.org/10.1016/j.ijhydene.2024.05.161.

[24] Fusaro R, Viola N. Design and integration of a cryogenic propellant subsystem for the hypersonic stratofly Mr3 vehicle. In: AIAA scitech 2020 forum. Vol. 1 PartF, 2020, http://dx.doi.org/10.2514/6.2020-1106.

[25] Sharifzadeh S, Verstraete D, Hendrick P. Cryogenic hydrogen fuel tanks for large hypersonic cruise vehicles. Int J Hydrog Energy 2015;40(37):12798–810. http://dx.doi.org/10.1016/j.ijhydene.2015.07.120.

[26] de Boer P, de Wit A, van Benthem R. Development of a liquid hydrogen-based fuel cell system for the HYDRA-2 drone. In: AIAA science and technology forum and exposition, AIAA sciTech forum 2022. 2022, http://dx.doi.org/10.2514/6.2022-0443.

[27] Winnefeld C, Kadyk T, Bensmann B, Krewer U, Hanke-Rauschenbach R. Modelling and designing cryogenic hydrogen tanks for future aircraft applications. Energies 2018;11(1):105. http://dx.doi.org/10.3390/en11010105.

[28] Ratnakar RR, Sun Z, Balakotaiah V. Effective thermal conductivity of insulation materials for cryogenic LH2 storage tanks: A review. Int J Hydrog Energy 2023;48(21):7770–93. http://dx.doi.org/10.1016/j.ijhydene.2022.11.130.

[29] Saias CA, Roumeliotis I, Goulos I, Pachidis V, Bacic M. Assessment of hydrogen fuel for rotorcraft applications. Int J Hydrog Energy 2022;47(76):32655–68. http://dx.doi.org/10.1016/j.ijhydene.2022.06.316.

[30] Nicolay S, Karpuk S, Liu Y, Elham A. Conceptual design and optimization of a general aviation aircraft with fuel cells and hydrogen. Int J Hydrog Energy 2021;46(64):32676–94. http://dx.doi.org/10.1016/j.ijhydene.2021.07.127.

[31] Onorato G, Proesmans P, Hoogreef MFM. Assessment of hydrogen transport aircraft. CEAS Aeronaut. J. 2022;13(4):813–45. http://dx.doi.org/10.1007/s13272-022-00601-6.

[32] Cipolla V, Zanetti D, Abu Salem K, Binante V, Palaia G. A parametric approach for conceptual integration and performance studies of liquid hydrogen short–medium range aircraft. Appl Sci 2022;12(14):6857. http://dx.doi.org/10.3390/app12146857.

[33] Millis MG, Tornabene RT, Jurns JM, Guynn MD, Tomsik TM, VanOverbeke TJ. Hydrogen fuel system design trades for high-altitude long-endurance remotely-operated aircraft. Technical report E-16800, 2009.

[34] Wang P, Ji L, Yuan J, An Z, Yan K, Zhang J. Modeling and optimization of composite thermal insulation system with HGMs and VDMLI for liquid hydrogen on orbit storage. Int J Hydrog Energy 2020;45(11):7088–97. http://dx.doi.org/10.1016/j.ijhydene.2019.12.110.

[35] Yin L, Yang H, Ju Y. Review on the key technologies and future development of insulation structure for liquid hydrogen storage tanks. Int J Hydrog Energy 2024;57:1302–15. http://dx.doi.org/10.1016/j.ijhydene.2024.01.093.

[36] Babac G, Sisman A, Cimen T. Two-dimensional thermal analysis of liquid hydrogen tank insulation. Int J Hydrog Energy 2009;34(15):6357–63. http://dx.doi.org/10.1016/j.ijhydene.2009.05.052.

[37] Kameni Monkam L, Graf von Schweinitz A, Friedrichs J, Gao X. Feasibility analysis of a new thermal insulation concept of cryogenic fuel tanks for hydrogen fuel cell powered commercial aircraft. Int J Hydrog Energy 2022;47(73):31395–408. http://dx.doi.org/10.1016/j.ijhydene.2022.07.069.

[38] Jiang W, Sun P, Li P, Zuo Z, Huang Y. Transient thermal behavior of multi-layer insulation coupled with vapor cooled shield used for liquid hydrogen storage tank. Energy 2021;231:120859. http://dx.doi.org/10.1016/j.energy.2021.120859.

[39] Joseph J, Agrawal G, Agarwal DK, Pisharady JC, Sunil Kumar S. Effect of insulation thickness on pressure evolution and thermal stratification in a cryogenic tank. Appl Therm Eng 2017;111:1629–39. http://dx.doi.org/10.1016/j.applthermaleng.2016.07.015.

[40] Xu W, Li Q, Huang M. Design and analysis of liquid hydrogen storage tank for high-altitude long-endurance remotely-operated aircraft. Int J Hydrog Energy 2015;40(46):16578–86. http://dx.doi.org/10.1016/j.ijhydene.2015.09.028.

[41] Cohen D, Mantell SC, Zhao L. The effect of fiber volume fraction on filament wound composite pressure vessel strength. Composites B 2001;32(5):413–29. http://dx.doi.org/10.1016/S1359-8368(01)00009-9.

[42] Brusa EGM, Nobile M. Assessment of a design method for composite overwrapped pressure vessels for hydrogen storage. Engineering systems design and analysis, Volume 1: Advanced energy systems, advanced materials, aerospace, automation and robotics, noise control and acoustics, and systems engineering, 2006, p. 321–33. http://dx.doi.org/10.1115/ESDA2006-95074.

[43] Çengel YA, Boles MA, Mehmet K. Thermodynamics: an engineering approach / Yunus A. Çengel, Michael A. Boles, Mehmet Kanoğlu. 9th ed.. New York: McGraw-Hill; 2018.

[44] Park SH, Antony J. Robust design for quality engineering and six sigma. Singapore: World Scientific; 2008.

[45] Dean A, Morris M, Stufken J, Bingham D. Handbook of design and analysis of experiments. 2015.

[46] of Heating Refrigerating AS, (ASHRAE) A-CEI. Aircraft. 2019 ASHRAE® handbook heating, ventilating, and air-conditioning applications. S-I ed.. American Society of Heating, Refrigerating and Air-Conditioning Engineers, Inc. (ASHRAE); 2019, 1–1.

[47] Standard temperature and pressure. Wikipedia 2024.